STRUCTURE STUDY OF $BACE_{0.85}Y_{0.15}O_{3-\Delta}$ AS SOLID STATE FUEL CELL MATERIAL

K. Krezhov[1, a)], D. Vladikova[2], G. Raikova[2], I. Genov[2], T. Malakova[1], D. Dimitrov[1], E. Svab[3], M. Fabian[3,4]

[1]*Institute forNuclear Research and Nuclear Energy, Bulgarian Academy of Sciences, Sofia, Bulgaria.*
[2]*Institute of Electrochemistry and Energy Systems, Bulgarian Academy of Sciences, Sofia, Bulgaria.*
[3]*Wigner Research Center for Physics, RISSPO, Hungarian Academy of Sciences, Budapest, Hungary.*
[4]*Center for Energy Research, Hungarian Academy of Sciences, Budapest, Hungary*

[a)]Corresponding author: krezhov@inrne.bas.bg

Abstract. The structural details of powder, dense and porous samples of $BaCe_{0.85}Y_{0.15}O_{3-\delta}$ (BCY15) used recently in an innovative monolithic design of SOFC were studied from multiple Rietveld analysis of neutron and x-ray diffraction patterns. The 3-layered monolithic assembly built from BCY15 material works as oxide ion conductor in the oxygen space, as proton conductor in the hydrogen area and as mixed conductor in the central membrane. We find that in all the samples of studied BCY15 based materials there are no indications of difference in crystallographic symmetry and the structure refinements did produce best agreement factors in orthorhombic Pnma space group.

INTRODUCTION

Solid oxide fuel cells (SOFCs) offer a promising green technology of direct conversion of the fuel chemical energy into electricity [1,2]. A typical SOFC is composed of four layers, three of which are ceramics. The ceramics used in SOFCs do not become electrically and ionic active until they reach high temperature ranging from 500 to 1,000 °C [3,4]. Reduction of oxygen into oxygen ions occurs at the cathode. The oxygen ions can diffuse through the solid oxide electrolyte to the anode where they can electrochemically oxidize the fuel. In this reaction, a water by-product is given off as well as two electrons. The generated electrons flow through an external circuit and the cycle then repeats as those electrons enter the cathode material again. The opposite process is also possible in case that the solid electrolyte is conducting protons. In this configuration (proton conducting SOFC) hydrogen is oxidized on the anode. The resulting from this process protons are transported through the electrolyte to the cathode, where they react with the oxygen, producing water as by-product.

Finding of appropriate combinations of electrolyte and electrode materials that provide both rapid ion transport across the electrolyte and electrode-electrolyte interfaces and efficient electrocatalysis of the oxygen reduction and fuel oxidation reactions remains a significant materials' challenge [5,6]. The advancement of highly efficient ion conduction materials is essential to the development of SOFC and other electrochemical devices such as batteries and hydrogen sensors. The quest is on solid oxide materials with high ionic conductivity while preserving structural stability at high temperatures. The oxygen-deficient ceramics of oxides with perovskite structure $A^{2+}B^{4+}O_3$, (A^{2+} = Ba, Sr, etc.; B^{4+} = Zr, Ce, Ti, Nb, etc.) are recognized among the most efficient materials that can be used as electrolytes or electrodes (metal-ceramic electrode structures) in SOFCs [1,5,6]. Oxygen-vacancy content in these ABO_3 oxides, wherein the B cation is partially substituted by a trivalent dopant, is relevant to proton-conducting oxides in which protons are introduced via the dissolution of hydroxyl ions at vacant oxygen sites [7,8]. In this study we report results from our neutron diffraction investigation on powder, dense and porous materials based on the composition $BaCe_{0.85}Y_{0.15}O_{3-\delta}$ (BCY15), which are tested currently in the new design of monolithic SOFC [9-12].

DUAL MEMBRANE FUEL CELL

The dual membrane fuel cell is a three compartment fuel cell based on a junction between a protonic ceramic fuel cell (PCFC) anode compartment (anode/electrolyte) and a SOFC cathode compartment (electrolyte/cathode) through a mixed proton and oxygen ion conducting porous composite ceramic membrane.

Fig. 1, a) shows the early stage of using BCY15 ($BaCe_{0.85}Y_{0.15}O_{3-\delta}$) as a proton conducting electrolyte material. Protons created at the anode progress toward the central membrane where they meet the oxide ions created at the cathode and produce water. Water is then evacuated through the interconnecting porous media of the central membrane. In this way hydrogen, oxygen and water are located in three independent compartments. This innovative concept has important advantages: the fuel and the oxidizer are not diluted; water does not inhibit the catalytic activity of the electrodes.

In the monolithic design, Fig. 1, b) the oxide ion conducting electrolyte is replaced with BCY15. Thus in oxygen flow (O_2) BCY15 is oxide ion conductor, in hydrogen flow (H_2) it is proton conducting. In the central membrane it is mixed ion conducting. This "single material" concept has better performance as fuel cell, but also as electrolyzer, since the material has a natural property to split water. The challenge is to develop the monolithic design as a device which works in reversible mode – as a fuel cell and as an electrolyzer.

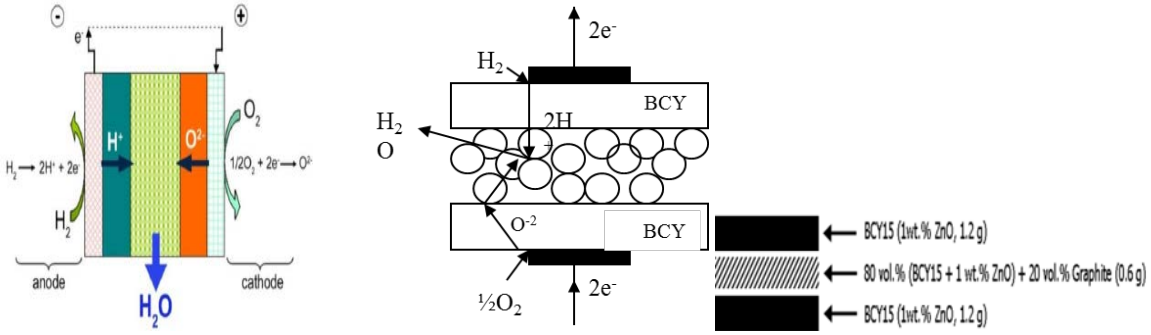

a) b)

FIGURE 1: a) Dual Membrane Fuel Cell (dmFC) ("classical" design): anode: Ni/BCY15; anode electrolyte: BCY15; composite central membrane: BCY15 + YDC15; cathode electrolyte: YDC15 ($Ce_{0.85}Y_{0.15}O_{1.925}$) ; cathode: LSCF ($La_{0.6}Sr_{0.4}CoFeO_{3-\delta}$); b) Monolithic dmFC [12]. The 3-layered monolithic assembly built from BCY15 material works as oxide ion conductor in the oxygen space, as proton conductor in the hydrogen area and as mixed conductor in the central membrane.

EXPERIMENTAL SECTION

BCY15 was prepared by auto-combustion technique starting from metal nitrates and using urea as reducing agent. Calcinations of the precursor at 1100-1150°C in inert atmosphere for complete CO_2 elimination ensured the production of single phase powder with desired chemical composition $BaCe_{0.85}Y_{0.15}O_{3-\delta}$ determined by ion coupled plasma analysis with dominating particle size of about 200 nm and minor degree of agglomeration. The BCY15 electrolyte support pellets (diameter/thickness = 20-25/1-1,3 mm) were prepared by cold pressing and sintering at a temperature of 1450°C. Initial characterization by X-ray diffraction, SEM and EDX shows BCY15 material with grain size 35-50 μm and density approximately 95% relatively to the theoretical density. Porous material was obtained by mixing thoroughly the powder BCY15 with graphite powder and firing the mixture at 1450°C.

The structural characterization of the polycrystalline BCY15 was carried out by laboratory X-ray diffraction using a Bruker D8 Advanced powder diffractometer in reflection mode with Bragg-Brentano geometry. The Topas-4.2 software was used to analyze the diffraction patterns collected with Cu Kα radiation (λ = 1.5418 Å) and LynxEye PSD detector at 20 °C in the angular range from 10° to 120° 2θ with a constant step 0.2° 2θ, 175 sec/point counting time. Phase identification was made with the Diffracplus EVA software using the International Centre for Diffraction Data (ICDD) PDF-2 database.

Neutron diffraction data were collected in the diffractometer PSD [13] of the Budapest Neutron Centre (λ = 1.069 Å, 3.60-114.0° in scattering angle 2θ, angular step size 0.1 °). The measurement was performed at 295 K on a powdered sample loaded in a thin-walled vanadium container. The diffraction data were analysed using the FULLPROF suite [14] by applying profile matching mode followed by full profile Rietveld refinement of the structural model. The tabulated coherent scattering lengths b_{coh} for Ba, Ce, Y and O were used: 5.07, 4.84, 7.75 and 5.803 fm, respectively. A pseudo-Voigt function was used for the simulation of the Bragg peaks profile and a fifth-degree polynomial function was applied for the fitting of the background.

RESULTS AND DISCUSSION

Fig. 2 shows an X-ray diffraction (XRD) pattern and neutron powder diffraction (NPD) patterns collected on some representative samples of the three types of BCY15 based material.

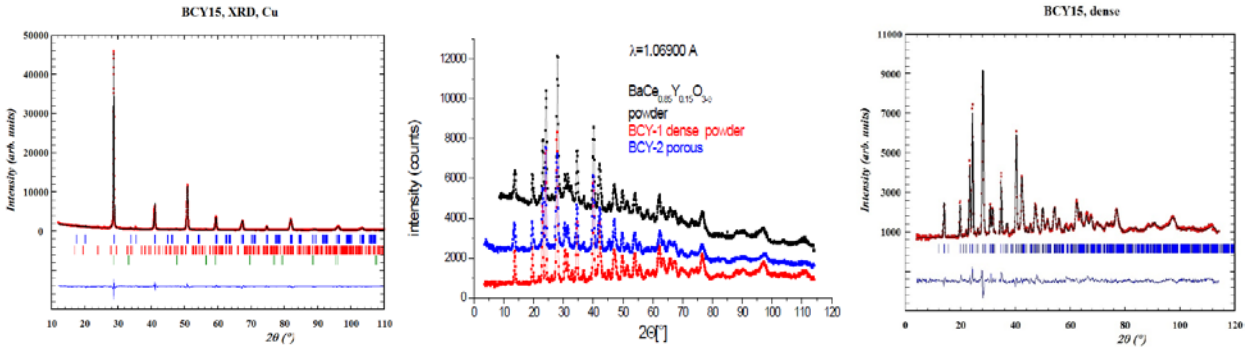

(a) (b) (c)

FIGURE 2. (**a)** Rietveld refined XRD pattern of a powder sample with nominal composition $BaCe_{0.85}Y_{0.15}O_{2.925}$ at 295 K. The rows of tick marks give the positions of the allowed in Pnma space group Bragg reflections for the main phase of BCY15 (upper) and the minority phases of $BaCo_3$ (middle) and CeO_2 (lower). The difference curve between the observed and calculated intensities in the full profile analysis is presented at the bottom; **(b)** NPD patterns of $BaCe_{0.85}Y_{0.15}O_{3-\delta}$ based samples at 295 K. The upper curve is from the sample denoted as powder and kept for three days in moist air. The patterns are vertically shifted to improve visibility; **(c)** Observed (crosses), calculated (continuous line), and difference (bottom) Rietveld NPD profiles of powdered dense BCY15 based material at 295 K. The row of tick marks gives the positions of Bragg reflections.

Figure 2,a) presents the X-ray experimental data, the final full profile refinement and the difference between them for a powder material $BaCe_{0.85}Y_{0.15}O_{2.925}$ at 295 K. The material measured was annealed in hydrogen-free atmosphere and kept stored under dry atmosphere. Traces of subsequently formed impurities CeO_2 and $CaCO_3$ were identified. Although the as-prepared substance was kept in a vessel under dry air, the revealed presence of minor phases of the order of 1,2 wt.% each one supports the claims that one major disadvantage of barium cerate based materials is their poor chemical stability in long term. Generally, in the presence of carbon dioxide barium carbonate and cerium (IV) oxides are produced in the reaction [3, 17] $BaCeO_3 + CO_2 \rightarrow BaCO_3 + CeO_2$.

Careful inspection of the NPD patterns shown in Fig. 2,b) did not reveal any indications of difference in crystallographic symmetry of the particular samples. The patterns could be indexed in rhombohedral space group R-3c and monoclinic symmetry space group I2/m. We have also checked for a mixture of two perovskite phases of R-3c and I2/m symmetry as recommended for this composition [15, 16]. However, in all the cases the structure refinements did not produce better agreement factors than in Pnma.

The multi-pattern mode of the FullProf program for simultaneous treatment of neutron and x-ray data sets was used to refine the structure and to determine the lattice parameters, atomic positions and thermal factors. We considered the undoped $BaCeO_3$ crystal structure as the starting structural model, with orthorhombic symmetry and space group Pnma; all the Bragg peaks of the diagram could be thus indexed. Yttrium atoms were introduced at random at 4b positions together with Ce, and the complementary occupancy factors were refined, constrained to a full occupancy. In the final refinement, the Ce/Y occupancy factors were unconstrained, indicating a slight deviation from the nominal 0.85:0.15 stoichiometry. Fig. 2,c) shows on the example of a powdered “dense” material the agreement between the observed and calculated NPD curves in the final multi pattern Rietveld fit. The structure parameters and the discrepancy factors describing the Rietveld fit quality are displayed in Table 1.

Fig.3 illustrates the attempt for refinement of the structure of the protonated sample. The extensive incoherent scattering of hydrogen from the hydroxyl groups is reflected by the steadily rising contribution to the background with decreasing to zero scattering angles. The fit is not of the required quality to allow for drawing up unambiguous conclusions for the structural details. By simultaneous treatment of multiple powder diffraction datasets obtained by present constant wavelength X-ray and neutron diffraction experiment the powder overlap problem is partially resolved in a Rietveld refinement. The effect of the multi pattern Rietveld analysis is effectively the deconvolution of the overlapping reflections by differing shifts in their relative positions. The medium resolution neutron powder data however have restricted the solution of the peak overlap problem in the structure models with protons.

Table 1 Refined structural parameters of $BaCe_{0.85}Y_{0.15}O_{2.925}$ in space group Pnma. Unit cell parameters (Å): a= 6.2089(9), b= 8.8292(6), c= 6.2066(8), volume (Å3) = 340.24(25). Agreement factors (%): R_{wp} =5.92, R_B = 3.66, $\chi 2$= 1.85. Estimated standard deviations are in parenthesis.

	x	*y*	*z*	*B, Å²*
Ba	0.0098(5)	0.25	-0.0028(7)	1.14(5)
Ce	0	0	0.5	0.56(6)
Y	0	0	0.5	0.56(6)
O1	0.5212(5)	0.25	-0.0792(7)	0.86(6)
O2	0.2674(4)	0.0395(7)	0.7249(7)	0.86(6)

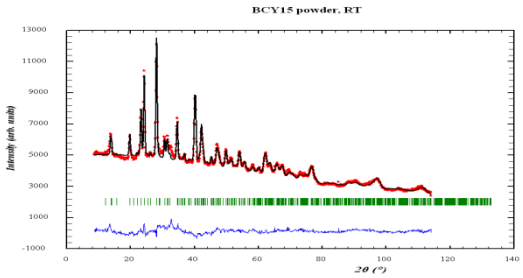

FIGURE 3 Observed (crosses), calculated (continuous line), and difference (bottom) Rietveld NPD profiles of protonated BCY15 based material at 295 K. The row of tick marks gives the positions of the allowed Bragg reflections.

In summary, the structure of $BaCe_{0.85}Y_{0.15}O_{3-\delta}$ (BCY15) material prepared by auto-combustion with following calcination at high temperature was investigated from full profile analysis of neutron and x-ray diffraction patterns collected at room temperature. The results on samples from powder, dense and porous BCY15 based materials used recently in a new monolithic design of SOFC show that the basic composition $BaCe_{0.85}Y_{0.15}O_{3-\delta}$ is crystallizing in the orthorhombic Pnma space group.

ACKNOWLEDGMENTS

This research is partially funded from the Bulgarian NFS under grant E02/3 2014. The study benefited from the bilateral cooperation of Hungarian and Bulgarian Academies of Sciences and the NMI3-II action (grant EU-FP7-NMI3 No.283883). We are indebted to Prof. D. Kovacheva from IGIC-BAS for the XRD experiments.

REFERENCES

1. T. A. Adams, J. Nease, D. Tucker and P. Barton, Ind. Eng. Chem. Res., **52**(9), 3089–3111 (2013).
2. L. Malavasi, C. A. J. Fisher and M. S. Islam, Chem. Soc. Rev., **39**(9), 4370-4387 (2010).
3. S. C. Singhal and K. Kendall (eds), High Temperature Solid Oxide Fuel Cells: Fundamentals, Design and Applications, Elsevier, 2003.
4. H. Iwahara, Y. Asakura, K. Katahira and M. Tanaka, J. Sol. St. Ionics **168**, 299-310 (2004).
5. A. Bassano, V. Buscaglia, M. Viviani, M. Bassoli, M. T. Buscaglia, M. Sennour, A. Thorel and P. Nanni, J. Sol. St. Ionics **180**, 168-174 (2009).
6. H. Iwahara, H. Uchida and K. Ogaki, J. Electrochem. Soc., **135**(2), 529-533 (1988).
7. H. Iwahara, T. Yajima and H. Uchida, J. Sol. St. Ionics **70/71**, 267-271 (1994).
8. K. S. Knight, Sol. St. Ionics **145**, 275−294, (20010.
9. Z. Stoynov, D. Vladikova and E. Mladenova, J. Sol. St. Electrochem., **17**, 555-560 (2013).
10. S. Thorel, A. Chesnaud, M. Viviani, A. Barbucci, S. Presto, P. Piccardo, Z. Ilhan, D. E. Vladikova and Z. Stoynov, J. Electrochem. Soc. **160**(4), F360-F366 (2013).
11. Patent N° 0550696000, March 17th, 2005, “Cellule de pile a combustible haute temperature a conduction mixte anionique et protonique”, International extension in 2006, Issue 2, Pennington, NJ (2009) 753.
12. A. Thorel, D. Vladikova, Z. Stoynov, A. Chesnaud, M. Viviani and S. Presto, “Fuel cell with monolithic electrolytes membrane assembly”, inventors. ARMINES patent #10 20120156573, June 17th, 2012.
13. http://www.bnc.hu
14. J. Rodriguez-Carvajal, Physica B **192**, 55 (1993); and https://www.ill.eu/sites/fullprof/
15. K. Takeuchi, C. K. Loong, J. W. Richardson, Jr. J. Guan, S. E. Dorris and U. Balachandran, J. Sol. St. Ionics **138**, 63–77, (2000).
16. C. L. Loong, M. Ozawa, K. Takeuchi and N. Koura, J. Alloys Compd., **408/412**, 1065–1070, (2006).
17. K. Przybylski, J. Prazuch, T. Brylewski, R. Amendola, S. Presto and M. Viviani, in Proc. Intern. Workshop Advances and Innovations in SOFCs, edited by D. Vladikova and Z. Stoynov (IEES, Sofia, 2011), pp. 62 -71.